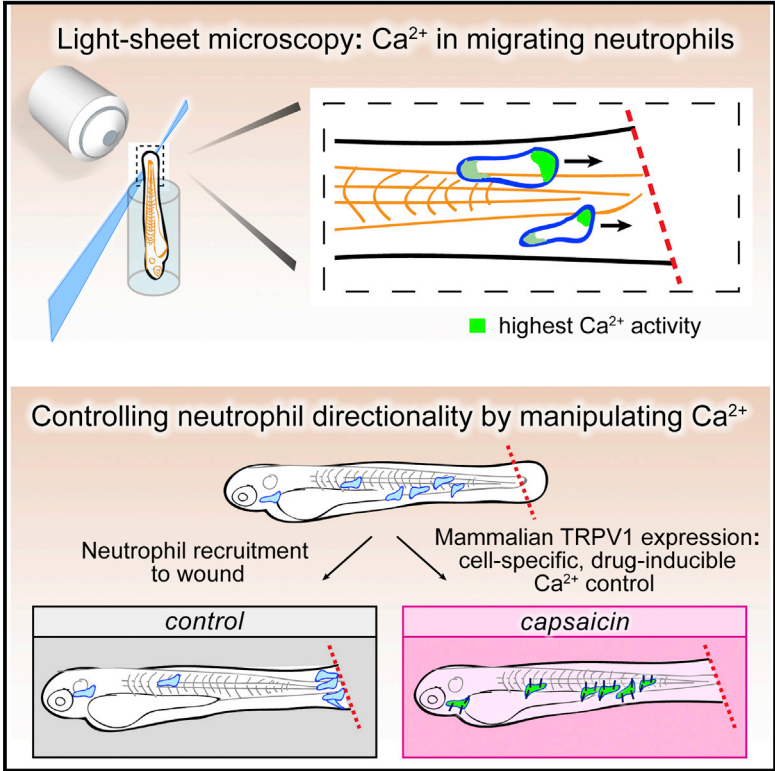


# Cell Reports

## Direct In Vivo Manipulation and Imaging of Calcium Transients in Neutrophils Identify a Critical Role for Leading-Edge Calcium Flux

### Graphical Abstract



### Authors

Rebecca W. Beerman, Molly A. Matty, Gina G. Au, Loren L. Looger, Kingshuk Roy Choudhury, Philipp J. Keller, David M. Tobin

### Correspondence

david.tobin@duke.edu

### In Brief

In vivo visualization of subcellular calcium dynamics in leukocytes has been challenging. Beerman et al. deploy light-sheet microscopy to identify leading-edge calcium enrichment in migrating zebrafish neutrophils. Calcium manipulation using cell-specific expression of a mammalian ion channel or pharmacological inhibition implicates leading-edge calcium in directional control of migrating neutrophils.

### Highlights

- Light-sheet microscopy in zebrafish reveals neutrophil calcium dynamics
- Migrating zebrafish neutrophils display enriched leading-edge calcium flux
- Mammalian TRPV1 allows drug-inducible, cell-specific regulation of calcium
- Leading-edge calcium signals can be instructive in setting neutrophil direction

# Direct In Vivo Manipulation and Imaging of Calcium Transients in Neutrophils Identify a Critical Role for Leading-Edge Calcium Flux

Rebecca W. Beerman,<sup>1</sup> Molly A. Matty,<sup>1,2</sup> Gina G. Au,<sup>1</sup> Loren L. Looger,<sup>3</sup> Kingshuk Roy Choudhury,<sup>4</sup> Philipp J. Keller,<sup>3</sup> and David M. Tobin<sup>1,5,\*</sup>

<sup>1</sup>Department of Molecular Genetics and Microbiology, Duke University, Durham, NC 27710, USA

<sup>2</sup>University Program in Genetics and Genomics, Duke University, Durham, NC 27710, USA

<sup>3</sup>Howard Hughes Medical Institute, Janelia Research Campus, Ashburn, VA 20147, USA

<sup>4</sup>Department of Biostatistics and Bioinformatics, Duke University, Durham, NC 27710, USA

<sup>5</sup>Department of Immunology, Duke University, Durham, NC 27710, USA

\*Correspondence: david.tobin@duke.edu

<http://dx.doi.org/10.1016/j.celrep.2015.11.010>

This is an open access article under the CC BY-NC-ND license (<http://creativecommons.org/licenses/by-nc-nd/4.0/>).

## SUMMARY

Calcium signaling has long been associated with key events of immunity, including chemotaxis, phagocytosis, and activation. However, imaging and manipulation of calcium flux in motile immune cells in live animals remain challenging. Using light-sheet microscopy for in vivo calcium imaging in zebrafish, we observe characteristic patterns of calcium flux triggered by distinct events, including phagocytosis of pathogenic bacteria and migration of neutrophils toward inflammatory stimuli. In contrast to findings from ex vivo studies, we observe enriched calcium influx at the leading edge of migrating neutrophils. To directly manipulate calcium dynamics in vivo, we have developed transgenic lines with cell-specific expression of the mammalian TRPV1 channel, enabling ligand-gated, reversible, and spatiotemporal control of calcium influx. We find that controlled calcium influx can function to help define the neutrophil's leading edge. Cell-specific TRPV1 expression may have broad utility for precise control of calcium dynamics in other immune cell types and organisms.

## INTRODUCTION

Intracellular calcium concentrations  $[Ca^{2+}]_i$  are tightly regulated; changes in the frequency and spatial distribution of  $[Ca^{2+}]_i$  affect multiple aspects of cellular activity. The first neutrophil behavior associated with calcium flux was identified almost 40 years ago (Boucek and Snyderman, 1976). However, subsequent analysis using alternative methods to visualize  $[Ca^{2+}]_i$  dynamics (Grienerberger and Konnerth, 2012; Tsien, 1980) were surprisingly divergent, with reports of enriched calcium at the front edge of migrating neutrophils (Sawyer et al., 1985), whole-cell calcium flux in migrating neutrophils with no calcium gradient (Marks

and Maxfield, 1990), and no detectable changes in neutrophil calcium levels during chemotaxis (Laffafian and Hallett, 1995). A low-amplitude leading-edge  $Ca^{2+}$  signal has been detected in polarized RAW cells in culture, a model system for macrophage chemotaxis, and this  $Ca^{2+}$  signal was shown to be essential for leading edge stability and ruffling (Evans and Falke, 2007). However, the presence of a leading-edge  $Ca^{2+}$  signal has not been demonstrated for any leukocyte in tissue.

Light-sheet microscopy enables whole-animal recordings of calcium dynamics in multiple cells simultaneously in small, transparent organisms (Keller et al., 2015). Zebrafish larvae are optically transparent and therefore ideal for studying immune-cell behaviors in real time and in whole animals (Renshaw and Trede, 2012). There is a high degree of genetic and functional conservation between the zebrafish and mammalian innate immune systems (Cambier et al., 2014; Harvie and Huttenlocher, 2015; Henry et al., 2013). Detailed characterizations of zebrafish neutrophils have motivated the establishment of new animal models for both neutrophil dysfunction, such as WHIM (Warts, Hypogammaglobulinemia, Infections, and Myelokathexis) syndrome, and bacterial infections, including *Pseudomonas aeruginosa* (Brannon et al., 2009; Clatworthy et al., 2009; Phennicie et al., 2010; Walters et al., 2010).

Here, we carry out high-resolution intravital recordings of calcium signaling in migrating neutrophils in whole, live vertebrates. Analysis of calcium dynamics using light-sheet microscopy reveals calcium enrichment at the leading edge of migrating neutrophils, rather than the classical model of highest calcium levels at the uropod (Wei et al., 2012). We describe a tool to perturb calcium dynamics in a cell-specific and controllable manner that has broad application for other immune cells. Cell-specific expression of a pharmacologically inducible calcium channel enables temporal and spatial regulation of calcium influx in live animals. We find that regulated neutrophil calcium flux is required for neutrophil migration and that calcium enrichment at the leading edge can help direct polarized migration. These approaches provide a platform for direct in vivo observation and manipulation of calcium dynamics in specific immune cell populations.

## RESULTS

### In Vivo Detection of Leading-Edge Calcium Enrichment in Migrating Neutrophils

To examine in vivo calcium dynamics during neutrophil recruitment, we coupled light-sheet microscopy with transgenic zebrafish lines expressing the genetically encoded calcium indicator GCaMP3 specifically in neutrophils. We expressed GCaMP3 specifically in neutrophils using the *LysC* promoter and generated *Tg(LysC:GCaMP3)* transgenic animals (Hall et al., 2007; Meijer et al., 2008; Oehlers et al., 2015; Tian et al., 2009). We amputated a small segment of the caudal fin, a well-established injury assay for inducing a local inflammatory response and robust neutrophil recruitment (Figure 1A) (Henry et al., 2013). We employed light-sheet fluorescence microscopy to image intracellular calcium with high spatial and temporal resolution in live animals 3 days post-fertilization (3 dpf) (Ahrens et al., 2013). To avoid artifacts associated with cell movement, we performed ratiometric imaging in animals that carried both GCaMP3 and a cytoplasmic red fluorescent protein, both driven under the same neutrophil-specific promoter, *Tg(LysC:GCaMP3; LysC:dsRed)* (Figure 1A).

Ratiometric analyses of neutrophils migrating toward the wound site revealed fluctuations in calcium across the migrating cells through time (Figures 1B and S1; Movie S1, part 1). In contrast to previous ex vivo observations in neutrophils (Laffafian and Hallett, 1995), but similar to observations in a macrophage model (Evans and Falke, 2007), the zone of highest calcium enrichment was consistently observed at the leading edge of migrating neutrophils in vivo (Figures 1C, 1D, and S2). The middle of the cell generally displayed the lowest calcium, and the lagging edge had transient instances of high calcium, but overall showed only slightly elevated calcium levels that did not reach those of the leading edge (Figures 1C, 1D, and S2). Stationary cells from these same animals failed to show any consistent subcellular calcium enrichment patterns over time (Figure S3; Movie S1, part 2). Thus, elevated calcium concentrations at the leading edge are a notable feature of migrating neutrophils in vivo.

### Neutrophils Exhibit Whole-Cell Calcium Flux at Wound Sites and during Phagocytosis

Neutrophils from *Tg(LysC:GCaMP3)* larvae also exhibited dramatic whole-cell calcium flux once they reached a distance of  $\sim 50$   $\mu\text{m}$  from the wound. To analyze calcium flux during recruitment, we carried out ventral fin wounding assays (Figure 2A). Neutrophils migrating toward the wound exhibited whole-cell calcium flux more often as they approached the site of injury compared to nearby neutrophils that were stationary (Figures 2B and 2C; Movie S2). The duration and frequency of whole-cell calcium signals were variable among the migrating neutrophils, lasting from  $\sim 30$  s to well over 1 min.

Calcium signaling has also been implicated in phagocytosis and ensuing downstream responses (Nunes and Demareux, 2010). We infected *Tg(LysC:GCaMP3)* larvae with fluorescently labeled *P. aeruginosa* and performed high-speed time-lapse imaging to capture individual phagocytosis events (Brannon et al., 2009). We found that larval neutrophils consistently exhibited an increase in intracellular calcium (lasting  $\sim 20$ – $30$  s) upon phago-

cytosis of *P. aeruginosa* (Figure 2D; Movie S2, parts 2–4). These studies highlight the complex nature of calcium signaling in vivo, as we observed distinct calcium signaling patterns for each neutrophil activity examined: leading-edge enrichment of calcium during migration, long whole-cell pulses of calcium influx at close proximity to a wound site, and relatively shorter whole-cell calcium pulses upon phagocytosis of *P. aeruginosa*.

### Pharmacological Control of Calcium Dynamics in Zebrafish Neutrophils via Expression of a Mammalian Ion Channel

To assess the functional relevance of these dynamics, we developed a generalizable method for directly manipulating calcium in immune cells in vivo. The cation channel TRPV1 is highly permeable to calcium, widely studied for its role in nociception, and was first identified based on its gating by capsaicin (Caterina et al., 1997). Administration of capsaicin to transgenic *Caenorhabditis elegans* expressing mammalian TRPV1 in specific sensory neurons can mediate neuronal depolarization (Tobin et al., 2002). We used the zebrafish *LysC* promoter to drive rat TRPV1 (rTRPV1) specifically in neutrophils, creating the stable line *Tg(LysC:rTRPV1-tdTomato)*. The critical amino acid residues required to confer capsaicin sensitivity to mammalian TRPV1 are not conserved in zebrafish, and wild-type zebrafish exhibit no behavioral response to capsaicin treatment (Caterina et al., 1997; Graham et al., 2013; Jordt and Julius, 2002). We found that intracellular calcium flux was specifically induced in neutrophils from *Tg(LysC:rTRPV1; LysC:GCaMP3)* larvae treated with capsaicin but was absent if treated with vehicle or in control larvae lacking the rTRPV1 channel and exposed to capsaicin (Figures 3A and 3B; Movie S3; data not shown). Prolonged capsaicin treatment resulted in sustained calcium entry in rTRPV1 positive neutrophils for up to 60 min (Figures 3A and 3B; Movie S3, part 2).

### Targeted Perturbation of Calcium Flux Inhibits Neutrophil Recruitment

We next developed a pulsed capsaicin delivery protocol that would maximize calcium influx while minimizing any potential cell death from prolonged depolarization (see Experimental Procedures). We amputated the caudal fin to induce neutrophil recruitment and then pulsed with capsaicin or vehicle. 2 hr post-wounding (2 hpw), neutrophils in the control groups (*Tg(LysC:dsRed)* larvae pulsed with capsaicin or *Tg(LysC:rTRPV1)* treated with vehicle) were recruited normally to the wound (Figures 3C and 3D). However, neutrophils in the *Tg(LysC:rTRPV1)* larvae pulsed with capsaicin failed to reach the wound site (Figures 3C and 3D), suggesting that disrupted calcium flux is sufficient to perturb recruitment. We also pretreated *Tg(LysC:rTRPV1)* larvae with capsaicin pulses before amputation and then followed the amputation with a 2-hr treatment in ethanol vehicle. Neutrophils from these pretreated animals exhibited partial to full recovery, showing that the suppression of neutrophil recruitment after capsaicin treatment is reversible (Figures 3C and 3D).

Neutrophil recruitment is associated with the immune response to bacterial infection with *P. aeruginosa* (Deng et al., 2013; Yang et al., 2012). We assessed whether the neutrophil-specific rTRPV1 could modulate neutrophil recruitment to

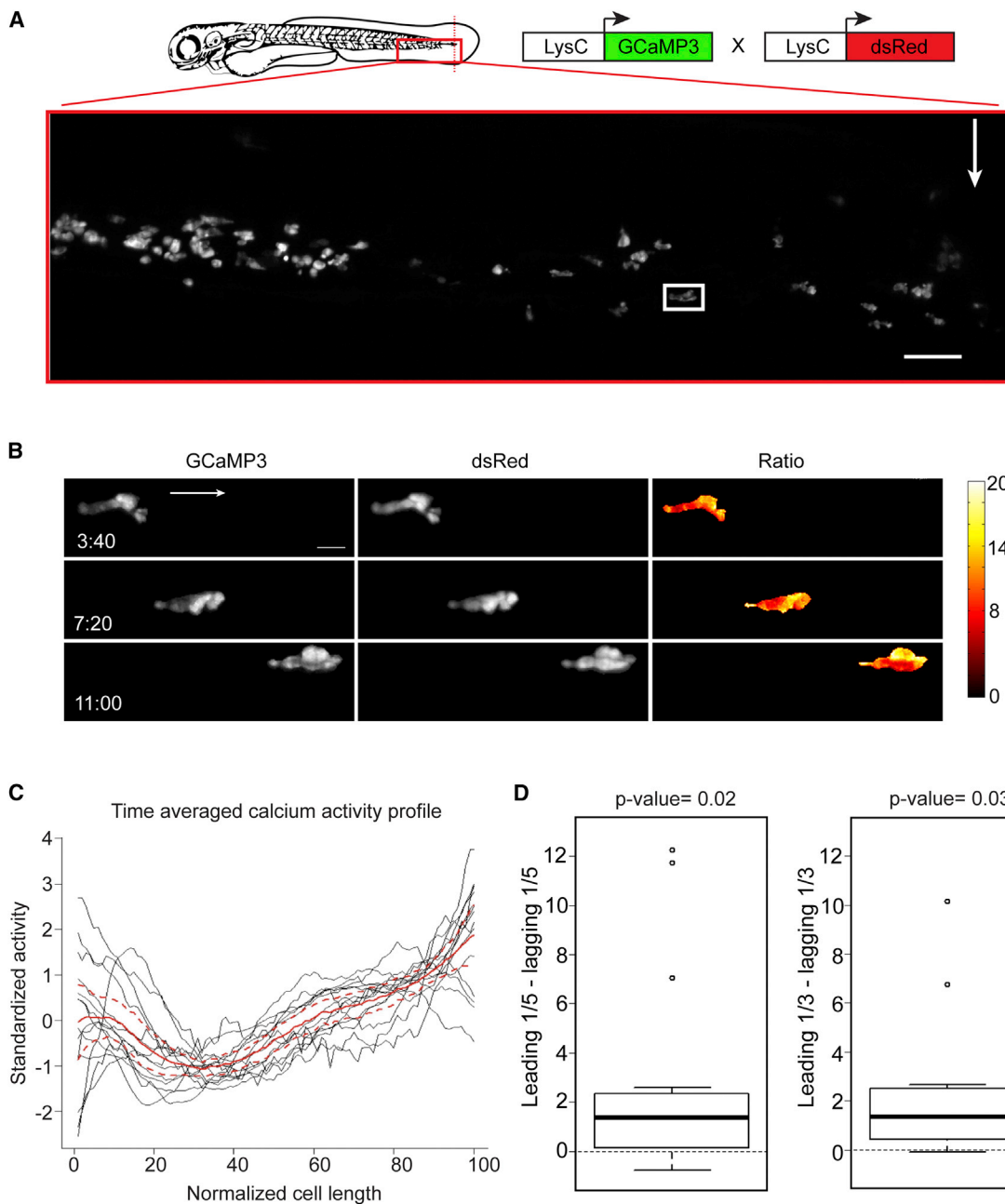


**Figure 1. Calcium Is Enriched at the Leading Edge of Migrating Neutrophils In Vivo**

(A) Illustration of a caudal fin amputation (red dotted line) in a double-transgenic larva *Tg(LysC:GCaMP3; LysC:dsRed)* with the field of view in the red box. White arrow indicates fin amputation, and white box highlights the neutrophil in the still frames in (B). Scale bar, 50  $\mu$ m.

(B) Maximum-intensity projections from time-lapse experiments with light-sheet fluorescence microscopy follow a single neutrophil migrating toward wound, displaying image data from each channel (GCaMP3 or dsRed) and resulting ratiometric image (GCaMP3/dsRed). Arrow indicates overall direction of migration.  $t = 0$  corresponds to 40 min post-wounding. Scale bar, 10  $\mu$ m.

(C) Time-averaged calcium activity profile across the length of a migrating neutrophil (normalized relative to direction of migration, where 0 is the lagging edge and 100 is the leading edge). Each neutrophil is graphed in black ( $n = 15$ , from four animals) with the mean profile (red line), bound by 95% confidence intervals (dashed red lines).

(D) Left box plot shows the difference between the average calcium signal at the leading and lagging edge (one-fifth of the length) for each neutrophil examined in (C). Middle line is the median, the box is the middle 50%, and the upper and lower bars indicate data range, with outliers as dots. Calculations were also repeated using the leading and lagging one-third of each cell (right box plot). Hypothesis that the average difference was positive was tested using a one-sample t test. See also [Figures S1–S3](#) and [Movie S1](#).

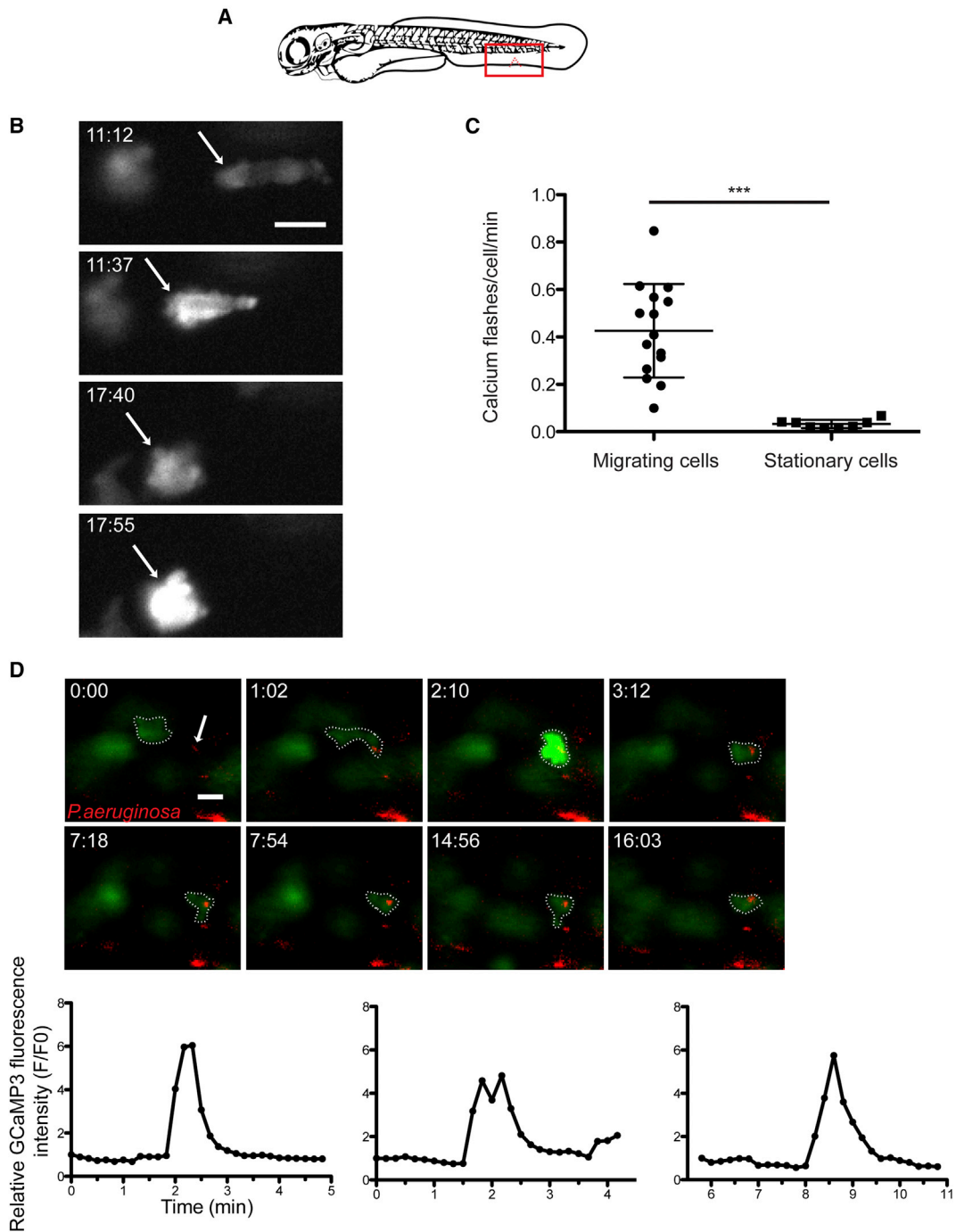


**Figure 2. Neutrophils Undergo Whole-Cell Calcium Flux at Sites of Injury and upon Phagocytosis of Bacteria**

(A) Cartoon of a ventral fin wound (red notch) and field of view during imaging (red square).

(B) Fluorescent images from a time-lapse following GCaMP3 expression in a neutrophil migrating toward a ventral fin wound in a *Tg(LysC:GCaMP3)* larva.  $t = 0$  corresponds to 5 min post-wounding. Arrow highlights a single neutrophil as it periodically flashes during migration toward a ventral wound.

(C) Mean number of whole-cell calcium flashes per cell per minute during the first hour post-wounding in migrating neutrophils and stationary neutrophils. Error bars are mean  $\pm$  SD. Mann-Whitney test \*\*\* $p < 0.0001$  ( $n = 15$  cells from five larvae for migrating cells, and  $n = 8$  cells from four larvae for stationary cells).

(D) Still frames from time-lapse capturing calcium flash upon LysC:GCaMP3 neutrophil (green) phagocytosis of *P. aeruginosa* (red). Dotted line surrounds the phagocytic neutrophil in each frame, and the arrow highlights bacteria that will be phagocytosed.  $t = 0$  corresponds to 30 min post-infection. Scale bars, 10  $\mu\text{m}$ . Graphs quantify the increase in relative fluorescence intensity from GCaMP3 ( $F/F_0$ ) during phagocytosis of PAO1. Left graph corresponds to the panels above, and the center and right graphs correspond to additional examples shown in [Movie S2](#), parts 3 and 4, respectively.

See also [Movie S2](#).

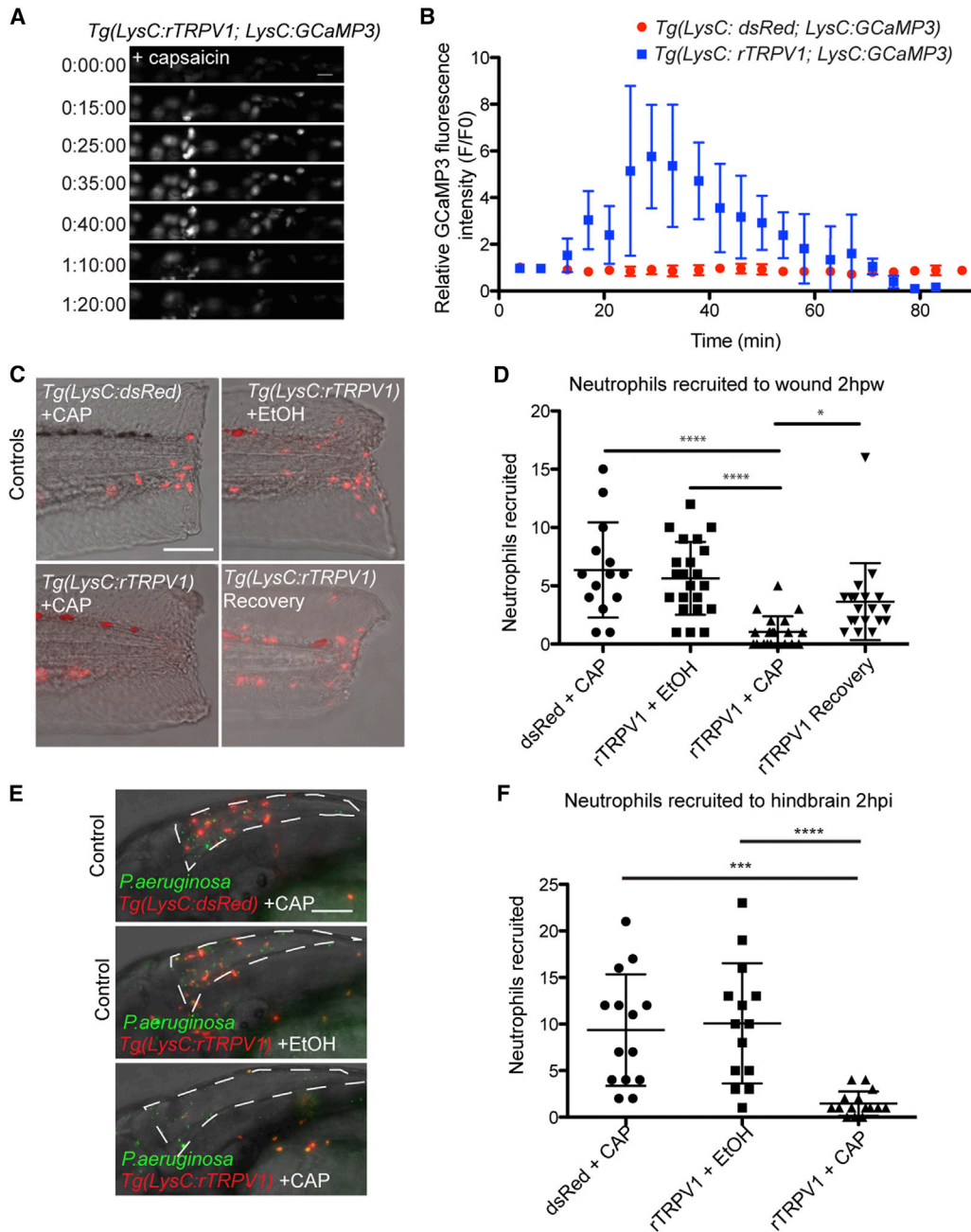


**Figure 3. Regulated Calcium Flux Is Required for Neutrophil Recruitment**

(A and B) Time-lapse experiment shows no change in GCaMP3 fluorescence in neutrophils from control *Tg(LysC:dsRed; LysC:GCaMP3)* larva after addition of capsaicin and increased GCaMP3 fluorescence in neutrophils from *Tg(LysC:rTRPV1; LysC:GCaMP3)* larva. (A) Selected still frames show GCaMP fluorescence in *Tg(LysC:rTRPV1; LysC:GCaMP3)* larva during extended exposure to capsaicin. t = 0 corresponds to 5 min after addition of capsaicin. Scale bar, 20  $\mu$ m. (B) Quantification of the relative GCaMP fluorescence intensity (F/F0) during extended capsaicin treatment (n = 5 neutrophils for each larva). Error bars are mean  $\pm$  SD. See also [Movie S3](#).

(C–F) *Tg(LysC:rTRPV1; LysC:GCaMP3)* or *Tg(LysC:dsRed; LysC:GCaMP3)* larvae were wounded (C and D) or infected with *P. aeruginosa* in the hindbrain (E and F) and briefly pulsed with capsaicin (CAP) or soaked in ethanol (EtOH) for 2 hr before neutrophil recruitment was quantified. Recovery *Tg(LysC:rTRPV1; LysC:GCaMP3)* larvae were pulsed with CAP before wounding, followed by EtOH soak for 2 hr to assess neutrophil recovery after capsaicin treatment (C and D). (C) Representative maximum-intensity projections show red-fluorescent neutrophils merged with bright field at 2 hr post-wounding. (E) Representative maximum-intensity projections show red-fluorescent neutrophils and green-fluorescent *P. aeruginosa* at 2 hr post-infection within the hindbrain ventricle outlined by white dashed line. Scale bars, 100  $\mu$ m. (D and F) Graphs display the number of neutrophils recruited for each larva. Error bars are mean  $\pm$  SD. Kruskal-Wallis test followed by Dunn's multiple comparison test: \*\*\*\*, adjusted p < 0.0001; \*\*\*, adjusted p = 0.0002; and \*, adjusted p = 0.014. Each experiment was carried out at least twice.

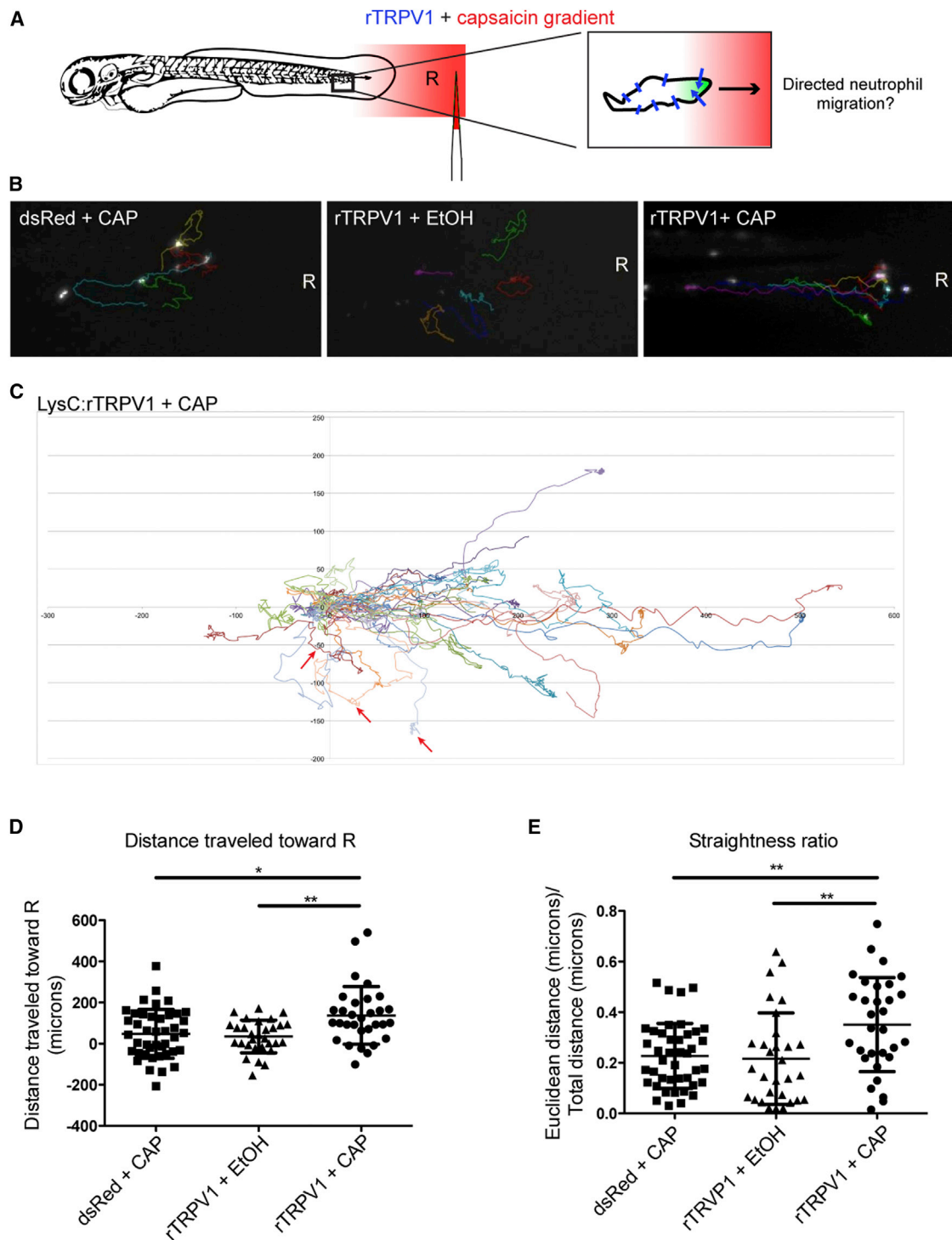


**Figure 4. A Capsaicin Gradient Directs rTRPV1-Neutrophil Motility**

(A) Injecting capsaicin (red) into surrounding agarose generates an intracellular calcium gradient (green) in neutrophils expressing rTRPV1 channels (blue lines). R indicates the reference point, defined as the initial point source of the gradient. Three experimental groups were imaged: *Tg(LysC:dsRed; LysC:GCaMP3)* larvae in a capsaicin gradient (dsRed+CAP), *Tg(LysC:rTRPV1; LysC:GCaMP3)* larvae in an ethanol gradient (rTRPV1+EtOH), or capsaicin gradient (rTRPV1+CAP). (B) Last frames from [Movie S4](#) show the tracks of individual neutrophils from each experimental group (quantified in D and E) relative to the reference point R at the focal point of the gradient.

(C) (x,y) coordinates for each neutrophil at every frame tracked within the *Tg(LysC:rTRPV1)* larvae exposed to a capsaicin gradient visually illustrate the directed motion toward the source. The track for each cell was normalized such that the starting (x,y) position was (0,0) for every cell. All units are  $\mu\text{m}$ . One larva from the

(legend continued on next page)

sites of infection. We infected *Tg(LysC:rTRPV1)* animals with *P. aeruginosa* in the hindbrain ventricle, an epithelial-lined compartment normally devoid of leukocytes, and quantified the number of neutrophils recruited 2 hr post-infection (2 hpi) (Figures 3E and 3F). Neutrophil recruitment to the *P. aeruginosa*-filled hindbrain was normal in both control groups but severely impaired in capsaicin-pulsed *Tg(LysC:rTRPV1)* larvae (Figures 3E and 3F). Thus, in both sterile inflammation and bacterial infection, excess calcium flux through capsaicin-gated rTRPV1 prevents normal neutrophil recruitment.

### Generation of a Capsaicin Gradient Drives Directed Neutrophil Migration

We next tested whether the observed calcium enrichment at the leading edge of neutrophils could instruct neutrophil movement in vivo. We sought to generate an intracellular calcium gradient by producing a directional capsaicin gradient, based on potential bias for channel gating on the side of the cell that first experiences an effective concentration of ligand (Figure 4A). We embedded *Tg(LysC:rTRPV1)* larvae in agarose and injected capsaicin proximal to the caudal fin. We observed sequential caudal to rostral fluorescence increases in GCaMP3-expressing neutrophils along the tail of *Tg(LysC:rTRPV1; LysC:GCaMP3)* larvae, suggesting that we could generate a gradient in the context of embedded larvae (Movie S4, part 1). However, the rapid neutrophil depolarization we observed with the high-dose gradient was incompatible with the slower time frame of endogenous neutrophil migration. Thus, we developed a lower-dose capsaicin gradient to attempt to experimentally induce leading-edge calcium enrichment in the absence of endogenous stimuli (Figure 4A).

The lower-dose capsaicin gradient had no effect on neutrophil migration in either control group (*Tg(LysC:dsRed)* plus a capsaicin gradient or *Tg(LysC:rTRPV1)* plus an ethanol gradient) (Figures 4B and S4; Movie S4). However, upon exposure to a capsaicin gradient, neutrophils expressing the rTRPV1 transgene migrated in a more directed trajectory toward the source (Figures 4B–4E; Movie S4), in the absence of any other stimulus. In comparison to controls, neutrophils in *Tg(LysC:rTRPV1)* animals traveled greater distances along straighter paths toward the highest point source of capsaicin (Figures 4D and 4E; Movie S4, parts 2–4). rTRPV1-neutrophils exhibited greater directionality toward the capsaicin gradient, but their mean velocities and total distances traveled were similar to those quantified from neutrophils in the control groups (Figures S4D and S4E). The similar velocities for random and directed neutrophil migration are consistent with previous recordings during baseline motility in interstitial tissue compared with chemotaxis toward a wound site (Yoo et al., 2010, 2011). Importantly, when we moved the point source of the capsaicin to the ventral side of the larva, migrating neutrophils

were redirected toward the new source, illustrating that the capsaicin gradient itself may help to define the direction of migration of rTRPV1-expressing neutrophils, even in the absence of any other stimuli (Figure S4C; Movie S4, part 5).

### Calcium Channels Influence Directed Neutrophil Motility

We next asked, via a reciprocal loss-of-function approach, whether calcium influx is required for chemotaxis in vivo. The calcium channel antagonist SKF 96365 displays activity against multiple calcium channels, including TRP channels and voltage-gated calcium channels (Harteneck et al., 2011; Merritt et al., 1990). Application of 20  $\mu$ M SKF 96365 to whole animals after caudal fin amputations compromised neutrophil recruitment (Figure 5A). We next modified these experiments, allowing a 30-min window after injury for chemotactic gradients to be established before applying the calcium channel antagonist, a time frame in which neutrophils have already begun to migrate toward the wound site (Niethammer et al., 2009; Movie S5). Neutrophils from larvae treated at these later time points were also compromised for recruitment, suggesting acute effects of the antagonist on neutrophil directional motility (Figure 5B).

To determine how limiting calcium influx acutely affects neutrophil behavior in vivo, we carried out detailed time-lapse microscopy and tracking in fin-amputated *Tg(LysC:GFP)* larvae. In a result consistent with the capsaicin gradient experiments, neutrophils in SKF 96365-treated larvae showed normal motility, traveling similar distances at similar velocities as control neutrophils (Figure 5C; Movie S5). However, administration of the calcium channel antagonist resulted in compromised directionality, with most neutrophils in treated animals exhibiting wandering, undirected patterns of migration (Figures 5C and 5D; Movie S5).

## DISCUSSION

Direct recording of intracellular calcium concentrations [ $\text{Ca}^{2+}$ ]<sub>i</sub> in migrating neutrophils was previously limited to ex vivo analyses (Boucek and Snyderman, 1976; Laffafian and Hallett, 1995; Marks and Maxfield, 1990; Sawyer et al., 1985), and observations have ranged from transient whole-cell flux to leading-edge calcium enrichment to no change in calcium flux at all (Laffafian and Hallett, 1995; Marks and Maxfield, 1990; Sawyer et al., 1985).

Using light-sheet microscopy and ratiometric imaging, we found enrichment of calcium at the leading edge of migrating neutrophils. This description is different from the high-resolution studies on calcium flux patterns in cultured chemotactic endothelial cells and fibroblasts, where there is high [ $\text{Ca}^{2+}$ ]<sub>i</sub> at the lagging edge and a low calcium concentration at the leading edge

rTRPV1 + CAP group was assessed after exposure to a ventrally centered gradient along the bottom of the animal and the three tracked cells from that animal are highlighted with red arrows.

(D and E) Graphs show the final distance traveled toward the reference point (D), and straightness ratio (E) for tracked neutrophils. Error bars are mean  $\pm$  SD. (D) Kruskal-Wallis test followed by Dunn's multiple comparison test: \*, adjusted p = 0.012 and \*\*, adjusted p value = 0.0075. (E) One-way ANOVA followed Tukey's multiple comparisons test: \*\*, adjusted p value = 0.0052 for dsRed+ CAP versus rTRPV1+CAP and \*\*, adjusted p value = 0.005 for rTRPV1+ EtOH versus rTRPV1+CAP. For each group, n  $\geq$  30 cells from  $\geq$  10 larvae.

See also Figure S4 and Movie S4.

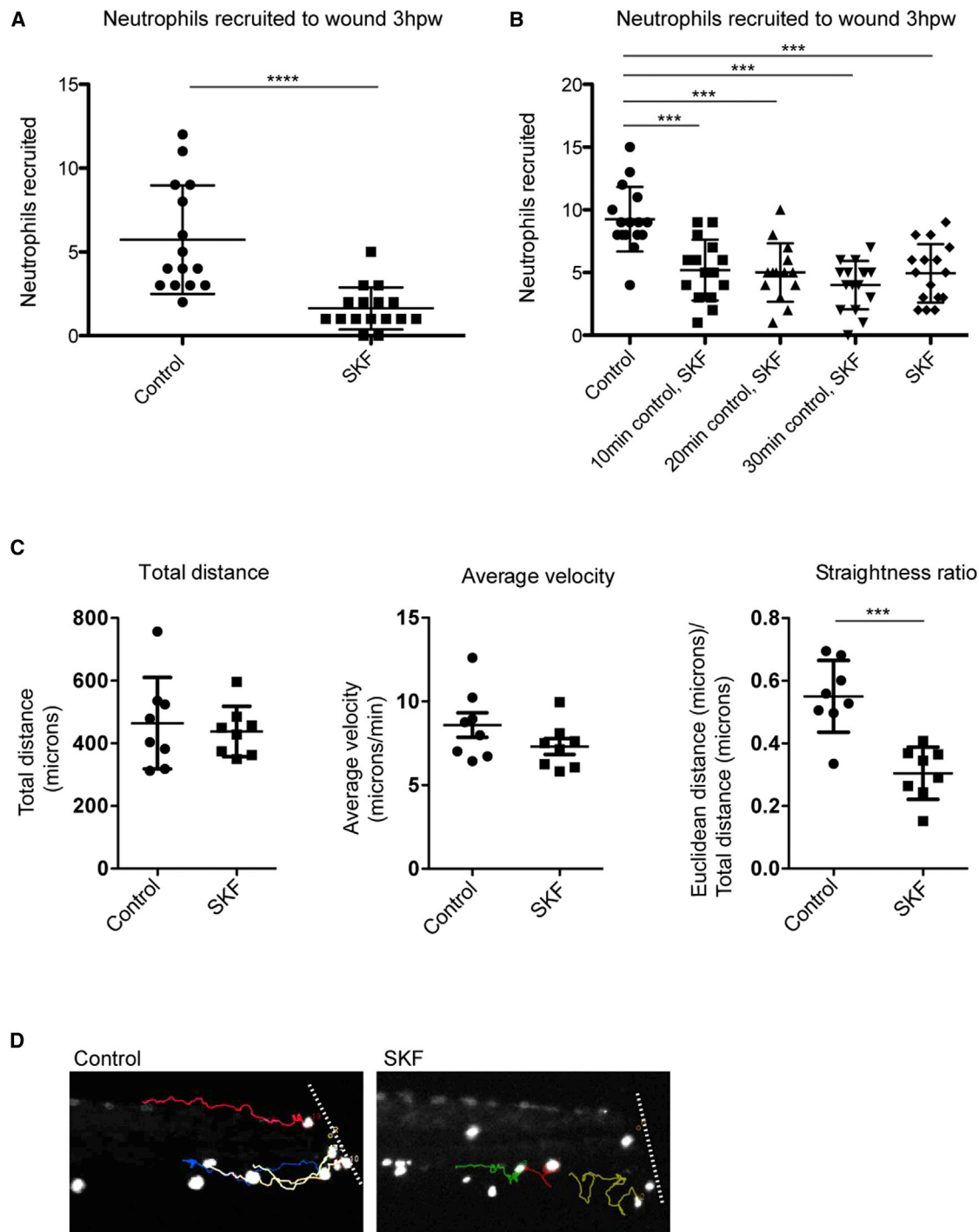


**Figure 5. Inhibition of Calcium Channels Disrupts Neutrophil Directionality during Recruitment**

(A–D) After caudal fin amputation, *Tg(LysC:GFP)* or *Tg(LysC:dsRed)* larvae were immediately treated with vehicle alone (control) or 20  $\mu$ M SKF 96365 (SKF), followed by quantification of neutrophil recruitment 3 hr post-wounding (A and B). (A) Error bars are mean  $\pm$  SD. Mann-Whitney test \*\*\*\* $p$  < 0.0001. (B) Groups of larvae were placed in control treatments for 10, 20, or 30 min before replacement of media with SKF for the remainder. Error bars are mean  $\pm$  SD. One-way ANOVA followed by Tukey’s multiple comparisons test \*\*\* $p$  < 0.001. Each experiment was carried out at least twice. (C and D) Immediately after wounding, larvae were mounted in agarose, immersed with either control or SKF, then imaged with time-lapse microscopy. (C) For the neutrophils tracked, graphs show their total distance traveled, average velocity, and straightness ratio. Total distance and straightness ratio error bars are mean  $\pm$  SD, and average velocity error bars are mean  $\pm$  SEM. *t* test, \*\*\* $p$  = 0.0002. For each group, *n* = 8 cells from two to three larvae. (D) Final frames from [Movie S5](#) show the tracks of individual neutrophils (quantified in C) near the amputated fin (approximated by the white line). See also [Movie S5](#).

punctuated with periodic sparks of localized  $[Ca^{2+}]_i$  (Tsai et al., 2014; Wei et al., 2009). In vivo analysis of neutrophils also showed moderately increased  $[Ca^{2+}]_i$  at the lagging edge, but the highest calcium signal was found at the leading edge. One unique feature of the neutrophils studied here was their fast pace. In vivo, chemotactic neutrophils moved at velocities up to 70 times greater than those recorded in the cited cell culture studies with other cell types.

The leading edge has been molecularly defined by a signaling cascade that translates an extracellular chemokine gradient into cytoskeletal rearrangements that promote movement (Falke and Ziemba, 2014). Many factors enriched at the leading edge of migrating cells also have direct or indirect associations with calcium, including phosphoinositide 3-kinases (PI3Ks) and PKC $\alpha$  (Ching et al., 2001; Evans and Falke, 2007; Hsu et al., 2000; Vossebeeld et al., 1997). PI3K activity has been localized to the leading edge of mouse neutrophils in cell culture and in zebrafish neutrophils in vivo, while PKC $\alpha$  is enriched at the leading edge of polarized murine macrophages (Evans and Falke, 2007; Nishio et al., 2007; Yoo et al., 2010). In macrophages, it has been hypothesized that a leading-edge calcium signal plays a role in directional control of cell migration (Evans and Falke, 2007; Falke and Ziemba, 2014).

The role of calcium signaling in immune cell phagocytosis and post-phagocytic vacuole trafficking has also generated conflicting results depending on the model system employed (Dewitt and Hallett, 2002; Jaconi et al., 1990; Lew et al., 1985; Marks and Maxfield, 1990; Murata et al., 1987; Nunes and Demarex, 2010; Sawyer et al., 1985). We have been able to directly image these dynamics in vivo. The transient rise in  $[Ca^{2+}]_i$  as *P. aeruginosa* is phagocytosed is similar to that observed for cultured human neutrophils phagocytosing opsonized antigens (Marks and Maxfield, 1990; Murata et al., 1987). The establishment of an in vivo model system for studying calcium dynamics during neutrophil phagocytosis should motivate greater understanding of how receptor-mediated phagocytosis of bacterial pathogens in animal models compares with cell culture models of opsonized antigens. These methods allow in vivo analysis of calcium flux in single immune cells for hours at high frame rates.

Although many regulators of calcium are used broadly in cell culture, they are largely incompatible with administration in a live organism. Cell-specific expression of TRPV1 provides a generalizable in vivo method to manipulate calcium dynamics in targeted immune cell subtypes. The rTRPV1-capsaicin system is pharmacologically inducible, titratable, and relatively sensitive to small variations, allowing for in vivo manipulation of subcellular calcium. By applying a low-dose capsaicin gradient across immobilized zebrafish larvae, neutrophils expressing the capsaicin-activated channel rTRPV1 were stimulated to move in the direction of the gradient. Asymmetric influx of calcium may be a key event in cell migration and may facilitate definition of the leading edge of some chemotactic cells. Additionally, we used a pharmacological loss-of-function approach to demonstrate an acute requirement for calcium channels in defining neutrophil directionality during an endogenous wounding response. Both the gain-of-function and loss-of-function manipulations of calcium influx resulted in reciprocal changes in directionality, but overall velocity remained largely unaffected, suggesting that

leading-edge calcium may be an important component of a neutrophil compass (Falke and Ziemba, 2014).

In summary, we have found that, in vivo, migrating neutrophils exhibit enriched calcium flux at the leading edge and that this pattern of intracellular calcium helps define the direction of movement. In addition, we describe a generalizable method for manipulating calcium directly in specific immune cells in vivo. The rTRPV1-capsaicin system requires no additional co-factors or prior knowledge of the functional endogenous calcium channels, thereby making it widely applicable as a method of interrogating the role of calcium signaling in many different cell types in whole animals.

## EXPERIMENTAL PROCEDURES

### Zebrafish Strains

All zebrafish husbandry and experimental protocols were performed in compliance with policies approved by the Duke University Institutional Animal Care and Use Committee. The transgenic lines *Tg(LysC:GCaMP3<sup>xt1</sup>)* and *Tg(LysC:rTRPV1-tdTomato<sup>xt4</sup>)* were made by injecting transposase mRNA and Tol2 containing DNA constructs into single-cell embryos, with additional details provided in Supplemental Experimental Procedures. *Tg(LysC:dsRed<sup>z250</sup>)* and *Tg(LysC:GFP<sup>z117</sup>)* have been described elsewhere (Hall et al., 2007).

### Time-Lapse Imaging

*Tg(LysC:GCaMP3)* larvae were imaged at 2 dpf for bacterial infection experiments, and all other transgenic larvae were imaged at 3 dpf. For microscopy, larvae were anesthetized in 0.016% Tricaine (MS-222) and immobilized in 1% low-melting-point agarose and imaged with a SiMView microscope (light-sheet microscopy), a Zeiss axio observer Z1, or Nikon TE-2000U. Additional experimental details are provided in Supplemental Experimental Procedures.

### Infections and Bacterial Preparations

*P. aeruginosa* (PAO1) carrying a constitutively expressed *mCherry* or *GFP* plasmid was grown in LB media supplemented with carbenicillin (200  $\mu$ g/ml) as previously described in (Brannon et al., 2009) and detailed in Supplemental Experimental Procedures.

### Quantitation of Calcium Flashes and Ratiometric Analyses

Light-sheet microscopy images were analyzed using maximum projections with background fluorescence subtracted. Details of ratiometric analyses are supplied in Supplemental Experimental Procedures. Whole-cell calcium flashes were quantified by manually scoring cells that displayed a notable increase in green fluorescence during the time-lapse session.

### Capsaicin and SKF 96365 Treatments

The final working capsaicin (Sigma) concentration was 20  $\mu$ M in 1.4% ethanol. Capsaicin gradient experiments were carried out by injecting 100  $\mu$ M capsaicin into the agarose, adjacent to the mounted larvae, followed by time-lapse microscopy. 10 mM SKF 96365 (Cayman Chemical) stock was made freshly in DMSO for each experiment. The final concentration was 20  $\mu$ M SKF 96365 in 0.5% DMSO. See Supplemental Experimental Procedures for additional details.

## SUPPLEMENTAL INFORMATION

Supplemental Information includes Supplemental Experimental Procedures, four figures, and five movies and can be found with this article online at <http://dx.doi.org/10.1016/j.celrep.2015.11.010>.

## ACKNOWLEDGMENTS

We thank Misha Ahrens, Sam Johnson, Wolfgang Liedtke, and Chao-Tsung Yang for helpful discussions and technical advice and support; Jörg Grandl,

Wolfgang Liedtke, Sam Moskowitz, and John Rawls for reagents and constructs; Jason Comparetto for assistance with video compilations; and Mark Cronan, Allison Rosenberg, and Jörn Coers for helpful discussions and critical comments on the manuscript. This work was supported by the Howard Hughes Medical Institute Janelia Visitor Program, a National Science Foundation Graduate Research Fellowship (M.A.M.), the Duke University Center for AIDS Research, an NIH-funded program (5P30 AI064518), and a Mallinckrodt Scholar Award, a Searle Scholar Award, a Vallee Foundation Young Investigator Award, and an NIH Director's New Innovator Award 1DP2-OD008614 (D.M.T.).

Received: July 11, 2015

Revised: September 21, 2015

Accepted: October 30, 2015

Published: December 3, 2015

## REFERENCES

- Ahrens, M.B., Orger, M.B., Robson, D.N., Li, J.M., and Keller, P.J. (2013). Whole-brain functional imaging at cellular resolution using light-sheet microscopy. *Nat. Methods* **10**, 413–420.
- Boucek, M.M., and Snyderman, R. (1976). Calcium influx requirement for human neutrophil chemotaxis: inhibition by lanthanum chloride. *Science* **193**, 905–907.
- Brannon, M.K., Davis, J.M., Mathias, J.R., Hall, C.J., Emerson, J.C., Crosier, P.S., Huttenlocher, A., Ramakrishnan, L., and Moskowitz, S.M. (2009). *Pseudomonas aeruginosa* Type III secretion system interacts with phagocytes to modulate systemic infection of zebrafish embryos. *Cell. Microbiol.* **11**, 755–768.
- Cambier, C.J., Takaki, K.K., Larson, R.P., Hernandez, R.E., Tobin, D.M., Urdahl, K.B., Cosma, C.L., and Ramakrishnan, L. (2014). Mycobacteria manipulate macrophage recruitment through coordinated use of membrane lipids. *Nature* **505**, 218–222.
- Caterina, M.J., Schumacher, M.A., Tominaga, M., Rosen, T.A., Levine, J.D., and Julius, D. (1997). The capsaicin receptor: a heat-activated ion channel in the pain pathway. *Nature* **389**, 816–824.
- Ching, T.T., Hsu, A.L., Johnson, A.J., and Chen, C.S. (2001). Phosphoinositide 3-kinase facilitates antigen-stimulated Ca<sup>2+</sup> influx in RBL-2H3 mast cells via a phosphatidylinositol 3,4,5-trisphosphate-sensitive Ca<sup>2+</sup> entry mechanism. *J. Biol. Chem.* **276**, 14814–14820.
- Clatworthy, A.E., Lee, J.S., Leibman, M., Kostun, Z., Davidson, A.J., and Hung, D.T. (2009). *Pseudomonas aeruginosa* infection of zebrafish involves both host and pathogen determinants. *Infect. Immun.* **77**, 1293–1303.
- Deng, Q., Sarris, M., Bennis, D.A., Green, J.M., Herbomel, P., and Huttenlocher, A. (2013). Localized bacterial infection induces systemic activation of neutrophils through Cxcr2 signaling in zebrafish. *J. Leukoc. Biol.* **93**, 761–769.
- Dewitt, S., and Hallett, M.B. (2002). Cytosolic free Ca<sup>2+</sup> changes and calpain activation are required for beta integrin-accelerated phagocytosis by human neutrophils. *J. Cell Biol.* **159**, 181–189.
- Evans, J.H., and Falke, J.J. (2007). Ca<sup>2+</sup> influx is an essential component of the positive-feedback loop that maintains leading-edge structure and activity in macrophages. *Proc. Natl. Acad. Sci. USA* **104**, 16176–16181.
- Falke, J.J., and Ziemba, B.P. (2014). Interplay between phosphoinositide lipids and calcium signals at the leading edge of chemotaxing amoeboid cells. *Chem. Phys. Lipids* **182**, 73–79.
- Graham, D.M., Huang, L., Robinson, K.R., and Messerli, M.A. (2013). Epidermal keratinocyte polarity and motility require Ca<sup>2+</sup> influx through TRPV1. *J. Cell Sci.* **126**, 4602–4613.
- Grienberger, C., and Konnerth, A. (2012). Imaging calcium in neurons. *Neuron* **73**, 862–885.
- Hall, C., Flores, M.V., Storm, T., Crosier, K., and Crosier, P. (2007). The zebrafish lysozyme C promoter drives myeloid-specific expression in transgenic fish. *BMC Dev. Biol.* **7**, 42.
- Harteneck, C., Klöse, C., and Krautwurst, D. (2011). Synthetic modulators of TRP channel activity. *Adv. Exp. Med. Biol.* **704**, 87–106.
- Harvie, E.A., and Huttenlocher, A. (2015). Neutrophils in host defense: new insights from zebrafish. *J. Leukoc. Biol.* **98**, 523–537.
- Henry, K.M., Loynes, C.A., Whyte, M.K., and Renshaw, S.A. (2013). Zebrafish as a model for the study of neutrophil biology. *J. Leukoc. Biol.* **94**, 633–642.
- Hsu, A.L., Ching, T.T., Sen, G., Wang, D.S., Bondada, S., Authi, K.S., and Chen, C.S. (2000). Novel function of phosphoinositide 3-kinase in T cell Ca<sup>2+</sup> signaling. A phosphatidylinositol 3,4,5-trisphosphate-mediated Ca<sup>2+</sup> entry mechanism. *J. Biol. Chem.* **275**, 16242–16250.
- Jaconi, M.E., Lew, D.P., Carpentier, J.L., Magnusson, K.E., Sjögren, M., and Stendahl, O. (1990). Cytosolic free calcium elevation mediates the phagosome-lysosome fusion during phagocytosis in human neutrophils. *J. Cell Biol.* **110**, 1555–1564.
- Jordt, S.E., and Julius, D. (2002). Molecular basis for species-specific sensitivity to “hot” chili peppers. *Cell* **108**, 421–430.
- Keller, P.J., Ahrens, M.B., and Freeman, J. (2015). Light-sheet imaging for systems neuroscience. *Nat. Methods* **12**, 27–29.
- Laffafian, I., and Hallett, M.B. (1995). Does cytosolic free Ca<sup>2+</sup> signal neutrophil chemotaxis in response to formylated chemotactic peptide? *J. Cell Sci.* **108**, 3199–3205.
- Lew, D.P., Andersson, T., Hed, J., Di Virgilio, F., Pozzan, T., and Stendahl, O. (1985). Ca<sup>2+</sup>-dependent and Ca<sup>2+</sup>-independent phagocytosis in human neutrophils. *Nature* **315**, 509–511.
- Marks, P.W., and Maxfield, F.R. (1990). Transient increases in cytosolic free calcium appear to be required for the migration of adherent human neutrophils. *J. Cell Biol.* **110**, 43–52.
- Meijer, A.H., van der Sar, A.M., Cunha, C., Lamers, G.E., Laplante, M.A., Kikuta, H., Bitter, W., Becker, T.S., and Spaink, H.P. (2008). Identification and real-time imaging of a myc-expressing neutrophil population involved in inflammation and mycobacterial granuloma formation in zebrafish. *Dev. Comp. Immunol.* **32**, 36–49.
- Merritt, J.E., Armstrong, W.P., Benham, C.D., Hallam, T.J., Jacob, R., Jaxa-Chamiec, A., Leigh, B.K., McCarthy, S.A., Moores, K.E., and Rink, T.J. (1990). SK&F 96365, a novel inhibitor of receptor-mediated calcium entry. *Biochem. J.* **271**, 515–522.
- Murata, T., Sullivan, J.A., Sawyer, D.W., and Mandell, G.L. (1987). Influence of type and opsonization of ingested particle on intracellular free calcium distribution and superoxide production by human neutrophils. *Infect. Immun.* **55**, 1784–1791.
- Niethammer, P., Grabher, C., Look, A.T., and Mitchison, T.J. (2009). A tissue-scale gradient of hydrogen peroxide mediates rapid wound detection in zebrafish. *Nature* **459**, 996–999.
- Nishio, M., Watanabe, K., Sasaki, J., Taya, C., Takasuga, S., Iizuka, R., Balla, T., Yamazaki, M., Watanabe, H., Itoh, R., et al. (2007). Control of cell polarity and motility by the PtdIns(3,4,5)P<sub>3</sub> phosphatase SHIP1. *Nat. Cell Biol.* **9**, 36–44.
- Nunes, P., and Demaurex, N. (2010). The role of calcium signaling in phagocytosis. *J. Leukoc. Biol.* **88**, 57–68.
- Oehlers, S.H., Cronan, M.R., Scott, N.R., Thomas, M.I., Okuda, K.S., Walton, E.M., Beerman, R.W., Crosier, P.S., and Tobin, D.M. (2015). Interception of host angiogenic signalling limits mycobacterial growth. *Nature* **517**, 612–615.
- Phennicie, R.T., Sullivan, M.J., Singer, J.T., Yoder, J.A., and Kim, C.H. (2010). Specific resistance to *Pseudomonas aeruginosa* infection in zebrafish is mediated by the cystic fibrosis transmembrane conductance regulator. *Infect. Immun.* **78**, 4542–4550.
- Renshaw, S.A., and Trede, N.S. (2012). A model 450 million years in the making: zebrafish and vertebrate immunity. *Dis. Model. Mech.* **5**, 38–47.
- Sawyer, D.W., Sullivan, J.A., and Mandell, G.L. (1985). Intracellular free calcium localization in neutrophils during phagocytosis. *Science* **230**, 663–666.

- Tian, L., Hires, S.A., Mao, T., Huber, D., Chiappe, M.E., Chalasani, S.H., Petreanu, L., Akerboom, J., McKinney, S.A., Schreier, E.R., et al. (2009). Imaging neural activity in worms, flies and mice with improved GCaMP calcium indicators. *Nat. Methods* 6, 875–881.
- Tobin, D., Madsen, D., Kahn-Kirby, A., Peckol, E., Moulder, G., Barstead, R., Maricq, A., and Bargmann, C. (2002). Combinatorial expression of TRPV channel proteins defines their sensory functions and subcellular localization in *C. elegans* neurons. *Neuron* 35, 307–318.
- Tsai, F.C., Seki, A., Yang, H.W., Hayer, A., Carrasco, S., Malmersjö, S., and Meyer, T. (2014). A polarized Ca<sup>2+</sup>, diacylglycerol and STIM1 signalling system regulates directed cell migration. *Nat. Cell Biol.* 16, 133–144.
- Tsien, R.Y. (1980). New calcium indicators and buffers with high selectivity against magnesium and protons: design, synthesis, and properties of prototype structures. *Biochemistry* 19, 2396–2404.
- Vossebeld, P.J., Homburg, C.H., Schweizer, R.C., Ibarrola, I., Kessler, J., Koenderman, L., Roos, D., and Verhoeven, A.J. (1997). Tyrosine phosphorylation-dependent activation of phosphatidylinositol 3-kinase occurs upstream of Ca<sup>2+</sup>-signalling induced by Fcγ receptor cross-linking in human neutrophils. *Biochem. J.* 323, 87–94.
- Walters, K.B., Green, J.M., Surfus, J.C., Yoo, S.K., and Huttenlocher, A. (2010). Live imaging of neutrophil motility in a zebrafish model of WHIM syndrome. *Blood* 116, 2803–2811.
- Wei, C., Wang, X., Chen, M., Ouyang, K., Song, L.S., and Cheng, H. (2009). Calcium flickers steer cell migration. *Nature* 457, 901–905.
- Wei, C., Wang, X., Zheng, M., and Cheng, H. (2012). Calcium gradients underlying cell migration. *Curr. Opin. Cell Biol.* 24, 254–261.
- Yang, C.T., Cambier, C.J., Davis, J.M., Hall, C.J., Crosier, P.S., and Ramakrishnan, L. (2012). Neutrophils exert protection in the early tuberculous granuloma by oxidative killing of mycobacteria phagocytosed from infected macrophages. *Cell Host Microbe* 12, 301–312.
- Yoo, S.K., Deng, Q., Cavnar, P.J., Wu, Y.I., Hahn, K.M., and Huttenlocher, A. (2010). Differential regulation of protrusion and polarity by PI3K during neutrophil motility in live zebrafish. *Dev. Cell* 18, 226–236.
- Yoo, S.K., Starnes, T.W., Deng, Q., and Huttenlocher, A. (2011). Lyn is a redox sensor that mediates leukocyte wound attraction in vivo. *Nature* 480, 109–112.